PHYSICAL REVIEW VOLUME 69, NUMBERS 5 AND 6 MARCH 1 AND 15, 1946

The Elastic, Piezoelectric, and Dielectric Constants of Potassium Dihydrogen Phosphate and Ammonium Dihydrogen Phosphate

W. P. MASON
Bell Telephone Laboratories, Murray Hill, New Jersey
(Received October 27, 1945)

Measurements have been made of all the elastic, piezoelectric, and dielectric constants of KDP and ADP crystals through temperature ranges down to the Curie temperatures. The piezoelectric properties agree well with Mueller's phenomenological theory of piezoelectricity provided the fundamental piezoelectric constant is taken as the ratio of the piezoelectric stress to that part of the polarization due to the hydrogen bonds. It is found that the dielectric properties of KDP agree well with the theory presented by Slater based on the interaction of the hydrogen bonds with the PO_4 ions. ADP undergoes a transition at $-125°C$ which results in fracturing the crystal. This transition cannot be connected with the H_2PO_4 hydrogen bond system which controls the dielectric and piezoelectric properties, for these lie on smooth curves that do not change slope as the transition temperature is approached. It is suggested that two separate and independent hydrogen bond systems are involved in ADP. The transition temperature and specific heat anomaly appear to be connected with hydrogen bonds between the nitrogens and the oxygens of the PO_4 ions, while the dielectric and piezoelectric properties are controlled by the H_2PO_4 hydrogen bonds.

I. INTRODUCTION

IT was first shown by Busch[1] that potassium dihydrogen phosphate KH_2PO_4 and several isomorphous salts, potassium dihydrogen arsenate KH_2AsO_4, ammonium dihydrogen phosphate $NH_4H_2PO_4$, and ammonium dihydrogen arsenate $NH_4H_2AsO_4$ exhibited phase changes at low temperatures. These crystals all exhibit phase changes at temperatures ranging from 91° absolute to 220° absolute temperature. It was established for potassium dihydrogen phosphate (which will be designated by the letters KDP) and potassium dihydrogen arsenate (KDA) by measuring the dielectric constants and the associated charge potential loops that these phase changes were of the ferroelectric type. Similar measurements of ammonium dihydrogen phosphate (ADP) and ammonium dihydrogen arsenate (ADA) failed to show ferroelectric properties on account of the sudden fracture of these crystals at temperatures above the ferroelectric Curie temperatures.

Measurements have been reported on the elastic properties of KDP,[2] and the piezoelectric constant of KDP,[3] over a temperature range, and some of the piezoelectric and elastic constants for all four crystals at room temperature,[4] but no complete measurements have been published of the properties of these crystals over temperature ranges down to the Curie temperatures. Such measurements, for small field strengths, are presented in the paper for two of these crystals KDP and ADP. The measurements for the dielectric constant of KDP are found to agree well with Slater's theory[5] based on the temperature variation of the position of the dipoles formed by the interaction of the hydrogens with PO_4 ions. However, the transformation occurring in ADP does not appear to be the ferroelectric type as envisaged by Slater for KDP. The measured piezoelectric relations agree with Mueller's[6] phenomenological theory of ferroelectricity if the fundamental piezoelectric constant is taken as the ratio of the piezoelectric stress to that part of the polarization due to hydrogen bonds.

[1] Georg Busch, "Neue Seignette Elektrika," Helv. Phys. Acta **11**, No. 3 (1938).
[2] W. Lüdy, "Der Einfluss der Temperature auf das Dynamisch Elastische Verhalten von Seignetteelektrika," Helv. Phys. Acta **20**, No. 8 (1942).
[3] W. Lüdy, "Piezoelectrizität von Kalium Phosphate," Zeits. f. Physik **113**, 302 (1939).
[4] H. Jaffe, "Piezoelectric studies of primary phosphates and arsenates," Abstract **D.3**, Bull. Am. Phys. Soc. (January 19, 1945).
[5] J. C. Slater, "Theory of the transition in KH_2PO_4," J. Chem. Phys. **9**, 16–33 (1941).
[6] H. Mueller, "Properties of Rochelle salt," Phys. Rev. **57**, 829–839 (1940).

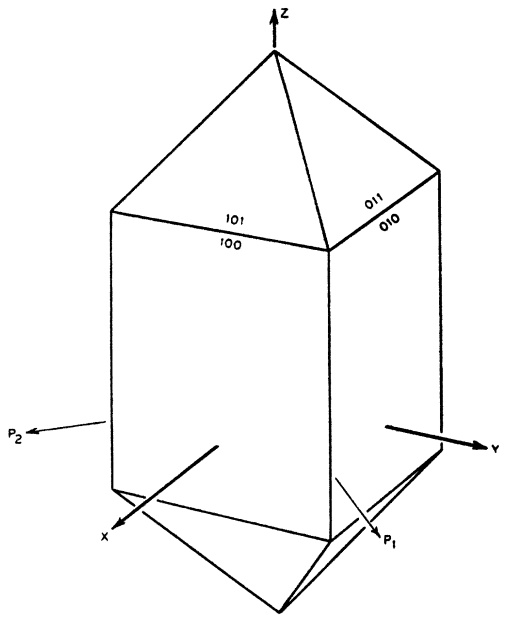

FIG. 1. Growth habit for ADP and KDP.

II. EXPRESSIONS FOR THE ELASTIC, DIELECTRIC, AND PIEZOELECTRIC EQUATIONS FOR ADP AND KDP CRYSTALS

All of the crystals of the isomorphous group, ADP, KDP, ADA, and KDA, crystallize in the tetragonal scalenohedral class with the habit shown by Fig. 1. The c or Z axis lies along the long direction of the crystal. This is an axis of fourfold alternating symmetry. The X and Y axes lie normal to the prism faces. These are axes of twofold symmetry. Since the properties of crystals cut normal to these two surfaces are identical except for sign, it is a matter of convention which axis is called X and which Y. The two diagonal axes, labelled P_1 and P_2 can be distinguished by piezoelectric tests, and P_1 has been taken as that axis along which a positive stress (tension) produces a positive charge at the positive (i.e., the upper) end of the Z axis. With the Z axis vertical and the P_1 axis toward the observer's right hand, the X axis has been taken as the axis which runs from front to back of the crystal and the Y axis from left to right (see Fig. 1). Etching studies by Dr. E. J. Armstrong show that an etch figure can be developed on the top surface as shown by Fig. 2 and the direction of the P_2 axis is in the line of the two spots.

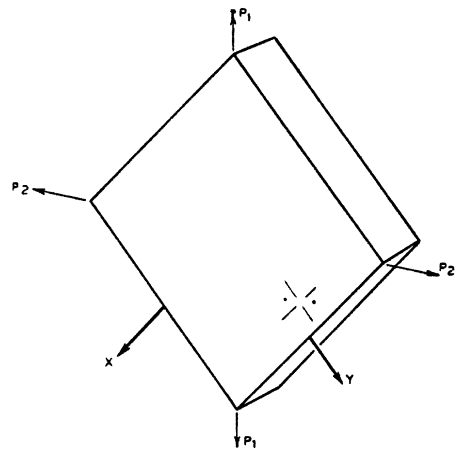

FIG. 2. Etch figures developed on ADP.

For a crystal having this symmetry Voigt[7] has shown that there will be six elastic compliances s_{11}, s_{12}, s_{13}, s_{33}, s_{44}, and s_{66}, two piezoelectric constants $d_{14}=d_{25}$ and d_{36}, and two dielectric constants $K_x=K_y$ and K_z. Voigt's method of writing the elastic and piezoelectric relations is

$$\begin{aligned}
-x_x &= s_{11}X_x+s_{12}Y_y+s_{13}Z_z;\\
-y_y &= s_{12}X_x+s_{11}Y_y+s_{13}Z_z;\\
-z_z &= s_{13}X_x+s_{13}Y_y+s_{33}Z_z;\\
-y_z &= s_{44}{}^E Y_z-d_{14}E_x;\\
-z_x &= s_{44}{}^E Z_x-d_{14}E_y;\\
-x_y &= s_{66}{}^E X_y-d_{36}E_z;\\
P_x &= \kappa_1{}^F E_x-d_{14}Y_z;\\
P_y &= \kappa_1{}^F E_y-d_{14}Z_x;\\
P_z &= \kappa_3{}^F E_z-d_{36}X_y;\\
\sigma_x &= P_x+E_x/4\pi;\\
\sigma_y &= P_y+E_y/4\pi;\\
\sigma_z &= P_z+E_z/4\pi;
\end{aligned} \tag{1}$$

where x_x, $\cdots$, x_y are the six strain components, X_x, $\cdots$, X_y the six stress components, E_x, $\cdots$, E_z the three field strengths along the three axes, P_x, $\cdots$, P_z the three polarizations along the three axes, and σ_x, $\cdots$, σ_z the surface charges normal to the three axes. s_{11} to s_{66} are the six

[7] Voigt, *Lehrbuch der Kristall Physik* (B. G. Teubner, Leipzig, 1910).

elastic compliances, d_{14}, d_{36} the two piezoelectric constants, κ_1^F, κ_3^F the two dielectric susceptibilities of the crystal free to move (i.e., with the stresses equal to zero). The compliances s_{44}^E, s_{66}^E are shown with a superscript E to indicate that they should be measured with the applied field constant or zero. By eliminating the polarizations, the last six equations can be written

$$\begin{aligned}\sigma_x &= K_1^F E_x/4\pi - d_{14} Y_z,\\ \sigma_y &= K_1^F E_y/4\pi - d_{14} Z_x,\\ \sigma_z &= K_3^F E_z/4\pi - d_{36} X_y,\end{aligned} \tag{2}$$

where K_1^F, K_3^F are the "free" dielectric constants which can be measured with the crystals unconstrained.

Voigt's relations can also be written by expressing the stresses in terms of the strains. These are obtained by solving the first six equations simultaneously, giving

$$\begin{aligned}-X_x &= c_{11}x_x + c_{12}y_y + c_{13}z_z; \quad -Y_z = c_{44}^E y_z - e_{14}E_x; \quad \sigma_x = K_1^C E_x/4\pi + e_{14}y_z;\\ -Y_y &= c_{12}x_x + c_{11}y_y + c_{13}z_z; \quad -Z_x = c_{44}^E z_x - e_{14}E_y; \quad \sigma_y = K_1^C E_y/4\pi + e_{14}z_x;\\ -Z_z &= c_{12}x_x + c_{13}y_y + c_{33}z_z; \quad -X_y = c_{66}^E x_y - e_{36}E_z; \quad \sigma_z = K_3^C E_z/4\pi + e_{36}x_y;\end{aligned} \tag{3}$$

where

$$c_{11} = \frac{\Delta^{11}}{\Delta}; \quad \cdots; \quad c_{33} = \frac{\Delta^{33}}{\Delta}; \quad \Delta = \begin{vmatrix} c_{11} & c_{12} & c_{13} \\ c_{12} & c_{22} & c_{13} \\ c_{13} & c_{13} & c_{33} \end{vmatrix};$$

Δ^{11} the determinant obtained by suppressing the first row and first column of Δ, etc.,

$$c_{44}^E = 1/s_{44}^E; \quad c_{66}^E = 1/s_{66}^E; \quad e_{14} = d_{14}/s_{44}^E = d_{14}c_{44}^E; \quad e_{36} = d_{36}/s_{66}^E = d_{36}c_{66}^E;$$
$$K_1^C = K_1^F - 4\pi(d_{14}e_{14}); \quad K_3^C = K_3^F - 4\pi(d_{36}e_{36});$$

K_1^C, K_3^C are the clamped dielectric constants of the crystal which are measured when the crystal is free from strain.

Voigt's relations express the stress, strain, and charge densities in terms of the applied field. It has been shown[8] that for a ferroelectric type crystal, the Voigt type parameters go through very wide changes when the crystal goes from a non-ferroelectric state to a ferroelectric state. However, if instead of the field strength, the polarization P or the charge density σ is used to relate the elastic terms to the piezoelectric terms it has been shown[6,8] for Rochelle salt that the elastic and piezoelectric constants are normal while the clamped dielectric constant shows a continuous variation with temperature. It is found advantageous to use a similar formulation for the constants of ADP and KDP.

For measuring purposes the formulation in terms of the surface charges is more advantageous since all the constants are directly determined by frequency and impedance measurements. Thus expressed the elastic constants correspond to the electrically open circuited condition while the Voigt constants correspond to the electrically short circuit condition. To obtain a piezoelectric constant that is independent of temperature requires relating the stress to that part of the polarization which depends on the temperature as will be shown later. The polarization constants are easily calculated from the charge constants by simple algebraic relations as will be discussed.

The two forms of the equations involving charge constants can be derived from Eqs. (1) and (3) by replacing E by σ. The form corresponding to Eq. (1) is

$$\begin{aligned}-x_x &= s_{11}X_x + s_{12}Y_y + s_{13}Z_z; \quad -y_z = s_{44}^\sigma Y_z - g_{14}\sigma_x; \quad E_x = \frac{4\pi\sigma_x}{K_1^F} + g_{14}Y_z;\\ -y_y &= s_{12}X_x + s_{11}Y_y + s_{13}Z_z; \quad -z_x = s_{44}^\sigma Z_x - g_{14}\sigma_y; \quad E_y = \frac{4\pi\sigma_y}{K_1^F} + g_{14}Z_x;\\ -z_z &= s_{13}X_x + s_{13}Y_y + s_{33}Z_z; \quad -x_y = s_{66}^\sigma X_y - g_{36}\sigma_z; \quad E_z = \frac{4\pi\sigma_z}{K_3^F} + g_{36}X_y;\end{aligned} \tag{4}$$

[8] W. P. Mason, "A dynamic measurement of the elastic, electric, and piezoelectric constants of Rochelle salt," Phys. Rev. 55, 775–789 (1939).

where

$$s_{44}^{\sigma}=s_{44}^{E}-d_{14}g_{14};\quad s_{66}^{\sigma}=s_{66}^{E}-d_{36}g_{36};\quad g_{14}=4\pi d_{14}/K_1^{F};\quad g_{36}=4\pi d_{36}/K_3^{F}.$$

The superscript σ over the elastic compliances s_{44} and s_{66} indicates that they are to be measured with the surface charge equal to zero. This is the value of the elastic constant measured mechanically or piezoelectrically in an air gap holder with a wide air gap. Similarly the form corresponding to Eq. (3) can be written,

$$\begin{aligned}
&-X_x=c_{11}x_x+c_{12}y_y+c_{13}z_z;\quad -Y_z=c_{44}^{\sigma}y_z-f_{14}\sigma_x;\quad E_x=\frac{4\pi\sigma_x}{K_1^{C}}-f_{14}y_z;\\
&-Y_y=c_{12}x_x+c_{22}y_y+c_{13}z_z;\quad -Z_x=c_{44}^{\sigma}z_x-f_{14}\sigma_y;\quad E_y=\frac{4\pi\sigma_y}{K_1^{C}}-f_{14}z_x;\\
&-Z_z=c_{13}x_x+c_{13}y_y+c_{33}z_z;\quad -X_y=c_{66}^{\sigma}x_y-f_{36}\sigma_z;\quad E_z=\frac{4\pi\sigma_z}{K_3^{C}}-f_{36}x_y;
\end{aligned}\tag{5}$$

where

$$c_{44}^{\sigma}=c_{44}^{E}+e_{14}f_{14};\quad c_{66}^{\sigma}=c_{66}^{E}+e_{36}f_{36};\quad f_{14}=4\pi e_{14}/K_1^{C}=g_{14}c_{44}^{\sigma};\quad f_{36}=4\pi e_{36}/K_3^{C}=g_{36}c_{66}^{\sigma}.$$

Other relations of interest that follow from Eqs. (4) and (5) are

$$g_{14}=f_{14}s_{44}^{\sigma};\quad g_{36}=f_{36}s_{66}^{\sigma};\quad \frac{4\pi}{K_1^{F}}=\frac{4\pi}{K_1^{C}}-g_{14}f_{14};\quad \frac{4\pi}{K_3^{F}}=\frac{4\pi}{K_3^{C}}-g_{36}f_{36}.\tag{6}$$

With all these interrelationships, all the different forms of expressing the piezoelectric relationships can be evaluated from one set of measurements.

If we wish to test whether the piezoelectric stress is proportional to the part of the polarization which varies with temperature and stress we can make use of the 6th and 9th equations of Eqs. (5), for example

$$-X_y=c_{66}^{\sigma}x_y-f_{36}\sigma_z,\quad E_z=\frac{4\pi\sigma_z}{K_3^{C}}-f_{36}x_y.\tag{7}$$

We can write that the total polarization is equal to a part Pz_0 which is independent of the temperature and strain and a part P_z' which varies with temperature and strain. Then the charge density σ_z is equal to

$$\sigma_z=\frac{E_z}{4\pi}+Pz_0+P_z'=\frac{E_z}{4\pi}(1+4\pi\kappa_{3_0})+P_z'=\frac{E_zK_{3_0}}{4\pi}+P_z',\tag{8}$$

where K_{3_0} is the temperature and strain independent part of the dielectric constant. Introducing this value into Eq. (7), the equations for the piezoelectric effect become

$$-X_y=c_{66}^{\sigma}x_y-f_{36}\left[\frac{E_zK_{3_0}}{4\pi}+P_z'\right],\tag{9}$$

$$E_z=\frac{4\pi}{K_3^{C}}\left(\frac{E_zK_{3_0}}{4\pi}+P_z'\right)-f_{36}x_y\quad\text{or}\quad E_z=\frac{4\pi}{(K_3^{C}-K_{3_0})}P_z'-\frac{f_{36}K_3^{C}}{K_3^{C}-K_{3_0}}x_y.\tag{10}$$

Introducing this value back in Eq. (9) the two piezoelectric equations become

$$E_z=\frac{4\pi P_z'}{K_3^{C}-K_{3_0}}-f_{36}^{*}x_y;\quad -X_y=\left(c_{66}^{\sigma}+\frac{f_{36}^{2}K_{3_0}K_3^{C}}{4\pi(K_3^{C}-K_{3_0})}\right)x_y-f_{36}^{*}P_z',\tag{11}$$

where f_{36}^{*} is a constant relating the piezoelectric stress X_y to the temperature variable portion of the polarization P_z'. Since we cannot suppress one portion of the polarization, these equations are not useful for measuring purposes, but if we have evaluated the charge constants, the proportionality of the piezoelectric stress to the polarization component P_z' can be tested by determining the ratio

$$f_{36}^{*}=\frac{X_y}{P_z'}=\frac{f_{36}K_3^{C}}{K_3^{C}-K_{3_0}}.\tag{12}$$

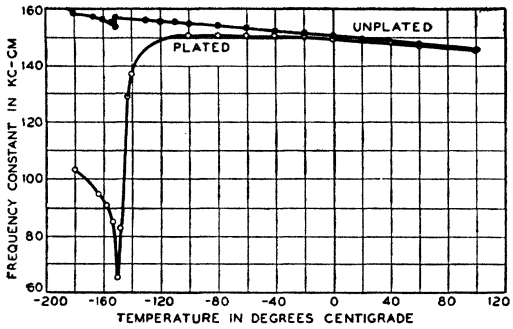

FIG. 3. Frequency constants of plated and bare 45° Z-cut KDP crystals.

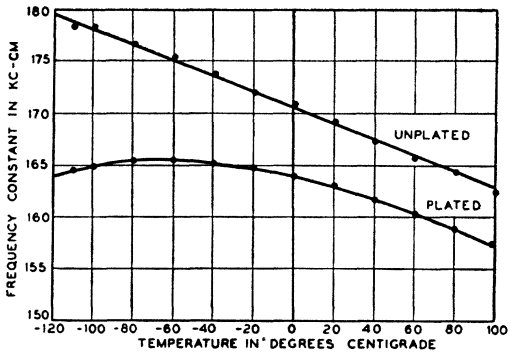

FIG. 4. Frequency constants of plated and bare 45° Z-cut ADP crystals.

III. MEASUREMENTS OF THE ELASTIC CONSTANTS OF ADP AND KDP OVER A WIDE TEMPERATURE RANGE

In order to measure the elastic constants of these crystals, seven oriented cuts of each type of crystal are used. When the crystals are plated and their resonant frequencies are measured, the short circuited elastic compliances s_{ij}^E are obtained as discussed in Appendix I. On the other hand, if the plating is removed and the crystals measured in an air gap holder with a large air gap, the open circuited constants s_{ij}^σ are obtained. Near the Curie point, there is a large difference between these constants, as can be seen from Fig. 3 which shows a measurement of the frequency constant of a KDP crystal cut normal to the Z axis, with its length at 45° from the X and Y axes. This crystal vibrates longitudinally. As can be seen the frequency constant of the plated crystal varies from 150 kilocycle-centimeters to 65 kilocycle-centimeters in the neighborhood of the Curie temperature (−151°C or +122°K). The frequency constant of the unplated crystal is a straight-line function of the temperature until the Curie temperature is reached. At that temperature a sudden discontinuity of the resonant frequency occurs larger than that occurring in Rochelle salt. This is caused by what Mueller[9] has called a "morphic" effect caused by a slight transformation of the crystal lattice.

Similar curves for a 45° Z-cut ADP crystal are shown by Fig. 4. At the temperature of −125°C (148°K) the crystal suddenly shatters into very small fragments. Even though the temperature was taken very slowly through this region it was not possible to prevent this shattering. Since the dielectric constant and the elastic compliance of the plated crystal do not increase sharply to a maximum, we conclude that the phase change is not one which involves the dipoles contributing to the dielectric and piezoelectric effect. It is a phase change of the first kind while that for KDP is a transition occurring over a range of temperatures.

Since it is simpler to measure the properties of a plated crystal, this has been done for the various cuts of ADP crystals and KDP crystals. In order to supplement such data near the Curie point of KDP, some measurements were made of the elastic constants of the unplated crystals cut normal to the Z axis.

Five of the crystals of each set were longitudinal crystals with their lengths 6 to 8 times their width and 12.5 times their thickness. Crystals of these dimensions have been found experimentally to be free of other modes of motion and to have a very small width correction to the frequency of the longitudinal mode. Hence the elastic constants are the values of Young's modulus appropriate for the plated crystal. The other two crystals of each set are X-cut and Z-cut crystals with one dimension long compared to the width and thickness. It is shown in the Appendix that such crystals produce shear modes of motion coupled to flexure modes. By properly dimensioning the crystals, the effect of the flexure can be eliminated and pure shear modes result. This allows one to measure the c_{44}

[9] H. Mueller, "Properties of Rochelle salt IV," Phys. Rev. **58**, 805–811 (1940).

TABLE I. Resonant frequencies of ADP.

Temperature in degrees cent.	X cut, $L=22.5°$ from Z axis $L=20.015$ mm $W=2.985$ mm $T=0.9$ mm plated resonant freq.	X cut, $L=45°$ from Z axis $L=20.00$ mm $W=2.96$ mm $T=0.97$ mm plated resonant freq.	X cut, $L=67.5°$ from Z axis $L=10.00$ mm $W=2.97$ mm $T=0.97$ mm plated resonant freq.	Z cut, $L=22.5°$ from X axis $L=19.69$ mm $W=2.94$ mm $T=20.96$ mm plated resonant freq.	Z cut, $L=45°$ from X axis $L=19.74$ mm $W=2.95$ mm $T=0.96$ mm plated resonant freq.	Z cut, $L=45°$ from X axis $L=19.74$ mm $W=2.95$ mm $T=0.96$ mm unplated resonant freq.
100	——	——	——	98,248	79,720	82,200
90	——	——	——	98,794	80,110	82,680
80	——	——	——	99,256	80,560	83,220
70	88,900	94,400	116,000	99,784	80,880	83,720
60	88,980	94,590	116,320	100,200	81,300	84,250
50	89,020	94,780	116,910	100,626	81,640	84,730
40	89,100	94,930	117,420	101,047	81,980	85,210
30	89,150	95,110	117,600	101,421	82,260	85,700
25	89,190	95,200	118,090	101,630	82,420	85,910
20	89,210	95,300	118,160	101,908	82,570	86,140
10	89,300	95,490	118,360	102,208	82,820	86,590
0	89,380	95,640	118,900	102,667	83,110	87,050
−10	89,450	95,810	119,290	102,817	83,280	87,420
−20	89,510	96,000	119,750	103,112	83,470	87,840
−30	89,590	96,200	119,910	103,366	83,620	88,190
−40	89,670	96,380	120,340	103,591	83,740	88,520
−50	89,720	96,555	120,890	103,800	83,850	88,890
−60	89,800	96,700	121,120	103,936	83,890	89,220
−70	89,880	96,900	121,320	104,040	83,900	89,510
−80	89,940	97,100	121,840	104,078	83,860	89,910
−90	90,010	97,290	122,250	104,063	83,730	90,220
−100	90,100	97,460	122,350	103,946	83,520	90,590
−110	90,190	97,620	122,750	103,771	83,340	90,950
−120	90,230	97,780	123,150	103,475	83,040	91,300

and c_{66} shear elastic constants directly. An alternate method used previously with Rochelle salt[8] was to use a thickness vibrating crystal dimensioned to eliminate extraneous modes of motion. However the dimensioning necessary for the face shear mode is less complicated and moreover the c_{44} and c_{66} constants are evaluated directly without allowing for the orientation necessary to drive the high frequency shear modes. By measuring high harmonics of the face shear mode, a frequency corresponding to a crystal very long compared with its width is obtained, and this provides a measurement free of width corrections for the shear modes.

Two of the length vibrating crystals are cut normal to the Z axis of the crystal with their lengths 22.5° and 45° from the X axis, respectively. The value of $s_{11}^{E'}$ (the inverse of Young's modulus) along the length of the crystal is given in the equation[8]

$$s_{11}^{E'}=s_{11}(\sin^4\varphi+\cos^4\varphi)+(2s_{12}+s_{66}^{E})\sin^2\varphi\cos^2\varphi. \quad (13)$$

Hence the two values of the frequency for these

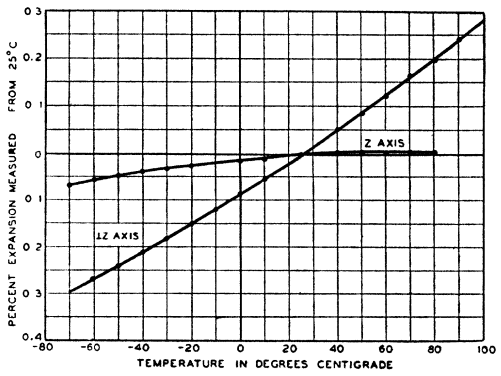

FIG. 5. Thermal expansion measurements for ADP.

TABLE II. Elastic compliances of ADP crystal cuts.

Temperature in °C	X cut, $L=22.5°$ from Z axis $s_{22}'^E$	X cut, $L=45°$ from Z axis $s_{22}'^E$	X cut, $L=67.5°$ from Z axis $s_{22}'^E$	Z cut, $L=22.5°$ from X axis $s_{22}'^E$	Z cut, $L=45°$ from X axis $s_{22}'^E$	Z cut, $L=45°$ from X axis $s_{22}'^\sigma$
100	——	——	——	3.70×10^{-12}	5.59×10^{-12}	5.26
90	——	——	——	3.67	5.50	5.20
80	——	——	——	3.63	5.49	5.12
70	4.40×10^{-12}	3.895×10^{-12}	2.575×10^{-12}	3.57	5.40	5.06
60	4.39	3.875	2.550	3.545	5.42	5.00
50	4.38	3.86	2.535	3.52	5.35	4.93
40	4.37	3.855	2.52	3.50	5.29	4.88
30	4.36	3.840	2.503	3.47	5.27	4.83
25	4.355	3.828	2.496	3.44	5.25	4.79
20	4.35	3.815	2.486	3.425	5.23	4.76
10	4.34	3.795	2.472	3.41	5.20	4.70
0	4.33	3.775	2.45	3.40	5.16	4.65
−10	4.315	3.765	2.43	3.36	5.13	4.60
−20	4.31	3.75	2.415	3.34	5.09	4.55
−30	4.305	3.73	2.404	3.335	5.07	4.53
−40	4.295	3.72	2.39	3.33	5.06	4.51
−50	4.29	3.715	2.37	3.32	5.05	4.47
−60	4.28	3.70	2.36	3.305	5.04	4.42
−70	4.275	3.685	2.35	3.295	5.045	4.41
−80	4.26	3.67	2.33	3.29	5.05	4.40
−90	4.25	3.655	2.32	3.295	5.06	4.37
−100	4.24	3.64	2.31	3.30	5.07	4.34
−110	4.23	3.625	2.29	3.31	5.12	4.33
−120	4.22	3.61	2.28	3.34	5.14	4.32

two crystals determine the s_{11} and $(2s_{12}+s_{66}^E)$ constants. The next three crystals had their major surfaces normal to the X axis and their lengths at approximately 22.5°, 45°, and 67.5° from the Y axis. The values of their Young's moduli are given by the equation[10]

$$s_{22}^{E'}=s_{11}\cos^4\psi+(2s_{13}+s_{44}^E)\sin^2\psi\cos^2\psi+s_{33}\cos^4\psi, \quad (14)$$

where ψ is the angle of the length measured from the Y axis.

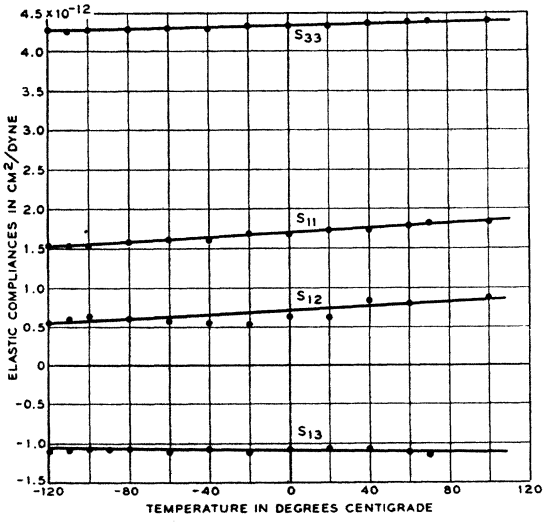

FIG. 6. Elastic compliances for ADP.

All of the crystals were lightly gold plated by the evaporation process and were held at their nodal point by a spring clamp. Five such crystals were put in one chamber[11] for which the temperature and humidity could be accurately controlled. For temperatures higher than room temperature, a heater in the central chamber was used to increase the temperature of the air. This air was circulated through the measuring chamber by means of a blower system and the

[10] This is proved for Rochelle salt in reference (8), Appendix I. The same proof holds for ADP if we let $s_{23}=s_{13}$; $s_{22}=s_{11}$.

[11] This chamber was designed and built by T. G. Kinsley and all the measurements over a wide temperature range have been taken by Kinsley and Mrs. J. Darr.

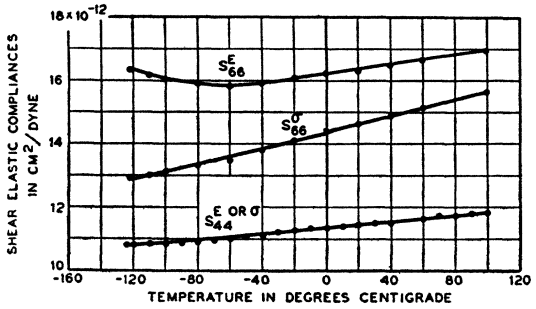

FIG. 7. Shear compliances for ADP crystals.

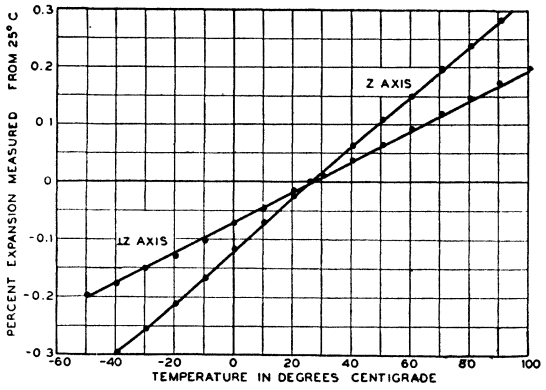

FIG. 8. Thermal expansion measurements for KDP.

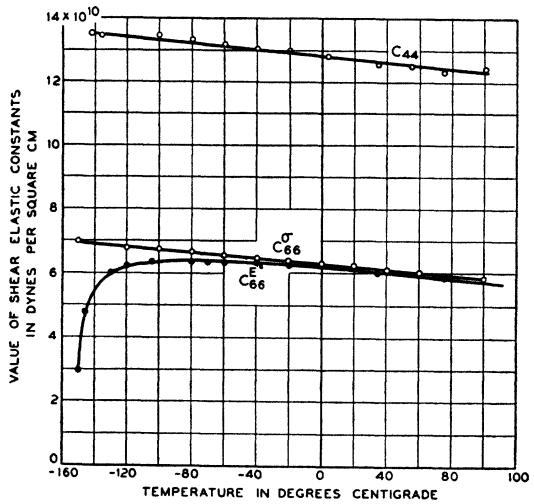

FIG. 9. Shear elastic constants of KDP.

temperature could be controlled by a thermostat on the heater system or on the blower system. For temperatures below the normal room temperature, dry ice or liquid nitrogen were placed in containers in the central chamber. The temperature in the measuring chamber was controlled by a thermostat on the blower system, and was measured by a mechanical thermometer or a thermocouple inserted near the crystal plates. With this arrangement temperatures from -165°C to $+250$°C can be maintained in the chamber. The humidity is kept low by the use of calcium chloride.

Table I shows the experimental data obtained for six vibrating ADP crystals. From these data, and the frequency equation

$$f=(1/2l)(1/\rho s_{22}')^{\frac{1}{2}}, \qquad (15)$$

it is possible to calculate the value of the elastic compliance s_{22}' (inverse of Young's modulus) at the temperatures given. To determine the true values however, it is necessary to know the temperature expansion along the two axes $X=Y$ and Z since this affects the values of l and ρ. The value of ρ has been found to be 1.804 by pycnometer methods.[12] The percentage expansions measured[13] from 25°C, for the two axes, are shown by Fig. 5. The expansion along the Z axis is considerably smaller and reaches a zero slope at temperatures of about 60° to 80°C. Table II gives values of elastic compliances for the six ADP crystal cuts over the temperature range measured. From these values and Eqs. (13) and (14), the value of s_{11}, s_{33}, $(2s_{12}+s_{66}^E)$ and $(2s_{12}+s_{44}^E)$ can be calculated. The values of s_{11} and s_{33} are shown by Fig. 6.

To obtain the values of the two shear constants s_{44}^E and s_{66}^E, two crystals were cut normal to the X and Z axes, respectively. These were dimensioned so that the shear resonance was obtained free from the other modes of motion (mostly flexural modes). For the 0° X cut, having the dimensions L (along Z) $=29.39$ mm; W (along Y) $=5.76$ mm; $T=1.025$ mm, there was a first resonance of 203,475 cycles, a third harmonic of 572,020 cycles, and a fifth harmonic of 953,500. These give an assymptotic frequency constant of 109.8 kilocycle centimeters, which results in a shear elastic compliance of $s_{44}^E=11.50\times10^{-12}$. Since the piezoelectric coupling is very small along the X axis, this is also within experi-

[12] This measurement was made by W. L. Bond.
[13] The expansion measurements have been made by Miss E. A. Baar.

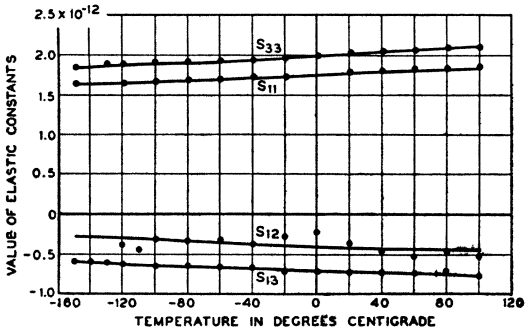

FIG. 10. Elastic compliances for KDP.

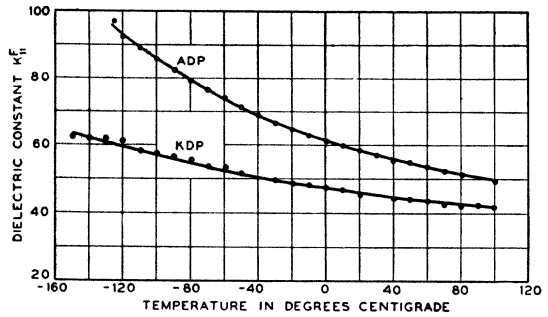

FIG. 11. Dielectric constants of ADP and KDP cut normal to the X axis.

mental error the value of the $s_{44}{}^{\sigma}$ constant. By measuring the fifth harmonic over a temperature range, the variation of the s_{44} constant was obtained as a function of temperature and is shown plotted by Fig. 7. In a similar manner a 0° Z-cut crystal having the dimensions $L=19.82$ mm along X, $W=2.96$ mm along Y and $T=1.11$ mm was found to have the first, fifth, and seventh harmonics of 321,260 cycles, 1,575,298 cycles, and 2,179,250 cycles, giving a frequency constant of 92.0 kilocycle centimeters for the shear mode. Over a temperature range, the corresponding values of $s_{66}{}^{E}$ are shown plotted in Fig. 7. By removing the plating another resonance curve was obtained and the corresponding elastic constant $s_{66}{}^{\sigma}$ is shown plotted by the full line of Fig. 7. It will be noted that the charge or "open circuited" elastic compliance is a linear function of the temperature while the potential or "short circuited" elastic compliance shows the effect of the variability of the electromechanical coupling with temperature. By using these values of the shear elastic compliances and the previously determined values of $(2s_{13}+s_{44}{}^{E})$ and $(2s_{12}+s_{66}{}^{E})$,

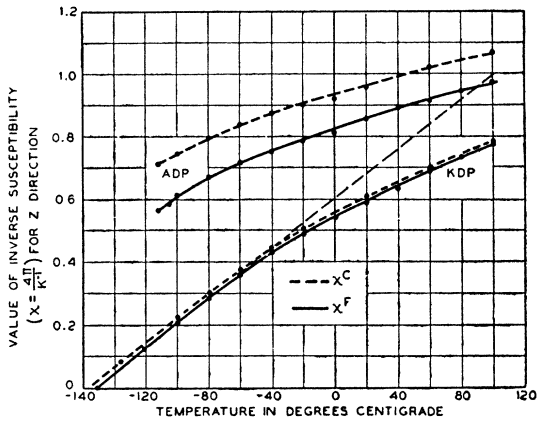

FIG. 12. Inverse of dielectric susceptibility for ADP and KDP cut normal to the Z axis.

the values of s_{12} and s_{13} can be evaluated and are shown plotted in Fig. 6. It will be noted that all of the open circuited elastic constants show a very regular variation with temperature. The direction in which the least temperature variation is to be expected for a longitudinal mode is along the Z axis. However, since no piezoelectric constant exists for driving such a vibration, this cannot be put to practical use.

A similar set of measurements has been made for all of the constants of potassium dihydrogen phosphate. In order not to burden the paper with too much detailed data, only the results are given. The changes in length of the two axes with temperature are shown by Fig. 8. The shear elastic constants of KDP, down to the Curie temperature, are shown by Fig. 9. On account of the large variation in the $c_{66}{}^{E}$ elastic constant this is plotted rather than its reciprocal $s_{66}{}^{E}$. As in ADP the coupling for an X-cut crystal is so small that no appreciable difference occurs between $c_{44}{}^{E}$ and $c_{44}{}^{\sigma}$. The remaining elastic constants of KDP are shown by Fig. 10. These are somewhat less than previous values of Lüdy,[2] who found values of 1.9×10^{-12} for s_{11} and 2.2×10^{-12} for s_{33} at room temperature. Other measurements of shear elastic constants $s_{44}{}^{E}$ and $s_{66}{}^{E}$ have recently been published by Jaffe.[4] For KDP he finds $s_{66}{}^{E}=15.5\times10^{-12}$ cm²/dyne at room temperature which is slightly less than the value of 16.4×10^{-12} found here. His values for ADP of $s_{44}=11.6\times10^{-12}$ and $s_{66}{}^{E}=16.6\times10^{-12}$ check well with the values found here for room temperature.

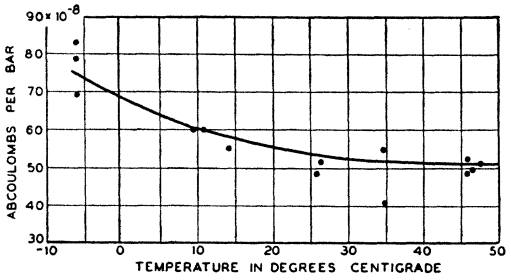

FIG. 13. Static measurements of the piezoelectric constant of KDP.

IV. DIELECTRIC AND PIEZOELECTRIC CONSTANTS OF ADP AND KDP

The dielectric constants of ADP and KDP have been measured by measuring the capacitances of the free crystals in a capacitance bridge at 1000 cycles. The results agree well with the original measurements of Busch.[1] The results for the two crystals normal to the X axis are shown by Fig. 11. On account of the high dielectric constants near the Curie point for KDP cut normal to the Z axis, the reciprocal susceptibility

$$\chi_3^F = 4\pi/(K_3^F - 1) \tag{16}$$

is plotted in Fig. 12. According to the theory discussed in the next section, this inverse susceptibility should be proportional to the difference in temperature between the actual temperature and the Curie temperature. This proportionality exists for about 100° above the Curie temperature, −151°C, but above this a bending off occurs which would be accounted for if we assume a temperature independent dielectric constant of value 4.5. This gives a "free" dielectric constant of

$$K_3^F = 4.5 + 3122/(T+151) \tag{17}$$

at any temperature above the Curie temperature of −151°C, and indicates that the dielectric constant is made up of a part which varies only slightly with temperature, and another part, due presumably to the hydrogen bonds, which varies inversely as the temperature difference. A similar equation fitting ADP is

$$K_3^F = 7.0 + 2670/(T+287), \tag{18}$$

indicating that the Curie temperature due to the hydrogen bonds is in the neighborhood of absolute zero. The clamped inverse susceptibilities are calculated from the piezoelectric constants and Eq. (3).

The piezoelectric constant of KDP was measured by W. L. Bond of these Laboratories in 1937. His method was a static one of suddenly removing a weight on a lever placed on both a quartz crystal and a KDP crystal and adjusting the position of the fulcrum until the voltage generated by one crystal balanced that from the other. From the piezoelectric equations given in section II, the constant of KDP can be compared with that of quartz, which is known quite precisely. Bond's results are given in Fig. 13. Because of the fact that KDP has a volume leakage much greater than that of quartz, this is not an accurate method and Bond's results are somewhat lower than those presented here which were measured by dynamic methods.

It is shown in the appendix that the separation of the resonant and anti-resonant frequencies of a longitudinally vibrating crystal is related to the electromechanical coupling in a crystal which depends on the ratio

$$k = d(4\pi/K^F s^E)^{\frac{1}{2}}, \tag{19}$$

where d is the piezoelectric constant for the longitudinal mode, K^F the "free" dielectric constant appropriate to the crystal, and s^E the inverse of Young's modulus for the crystal. For a 45° Z cut this becomes

$$k = \frac{d_{36}}{2}(4\pi/K_3^F s_{11}^{E'})^{\frac{1}{2}} = \frac{d_{36}}{2}\left[4\pi \Big/ K_3^F\left(\frac{s_{11}+s_{12}}{2}+\frac{s_{66}^E}{4}\right)\right]^{\frac{1}{2}}, \tag{20}$$

where $s_{11}^{E'}$ is the inverse of the short circuited

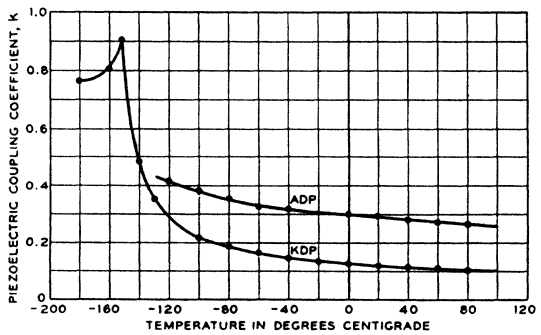

FIG. 14. Coupling constants of ADP and KDP.

value of Young's modulus. The frequency of a plated crystal is controlled by

$$f_p=(1/2l)(1/\rho s_{11}^{E'})^{\frac{1}{2}}, \tag{21}$$

while that of a bare crystal is controlled by

$$f_b=(1/2l)(1/\rho s_{11}^{\sigma})^{\frac{1}{2}}. \tag{22}$$

Hence, taking the ratio and introducing the results of Eq. (3)

$$\left(\frac{f_p}{f_b}\right)^2=\frac{s_{11}^{\sigma'}}{s_{11}^{E'}}=\frac{\frac{s_{11}+s_{12}}{2}+\frac{1}{4}s_{66}^{\sigma}}{\frac{s_{11}+s_{12}}{2}+\frac{1}{4}s_{66}^{E}}$$

$$=\frac{\frac{s_{11}+s_{12}}{2}+\frac{1}{4}(s_{66}^{E}-d_{36}g_{36})}{\frac{s_{11}+s_{12}}{2}+\frac{1}{4}s_{66}^{E}}=1-\frac{d_{36}g_{36}}{4s_{11}^{E'}}. \tag{23}$$

But since $g_{36}=4\pi d_{36}/K_3^F$, we have

$$1-\frac{d_{36}g_{36}}{4\pi s_{11}^{E'}}=1-\frac{d_{36}^2}{4}\left(\frac{4\pi}{K_3^F s_{11}^{E'}}\right)$$

$$=1-k^2=\left(\frac{f_p}{f_b}\right)^2. \tag{24}$$

Hence, the piezoelectric coupling k can be evaluated from the data of the last two crystals of Table I and is shown plotted in Fig. 14 for ADP. Similarly the data of Fig. 3 gave the coupling for KDP, which is also shown on Fig. 14. It will be noted that the coupling rises to 92 percent at the Curie temperature and remains high in the ferroelectric region for small applied fields.

TABLE III. Piezoelectric constants of ADP.

Temperature in °C	$d_{36}\times10^8$	$e_{36}\times10^{-4}$	$g_{36}\times10^8$	$f_{36}\times10^{-4}$	K_3^C	$f_{36}^*\times10^{-4}$
100	129.5	7.62	117	7.47	12.9	16.3
80	132.5	7.82	116	7.55	13.0	16.3
60	136.0	8.14	116	7.67	13.3	16.2
40	142.0	8.61	117.5	7.87	13.6	16.2
20	148	9.04	118.5	8.09	14.0	16.2
0	155	9.54	120	8.37	14.4	16.3
−20	161	10.0	119	8.44	14.9	16.0
−40	170	10.65	121	8.75	15.4	16.1
−60	180	11.32	122	8.94	16.0	15.9
−80	198	12.4	125	9.35	16.7	16.1
−100	207	12.9	126	9.6	17.3	16.1
−110	242	14.9	130	10.0	18.2	16.3
−120	261	15.4	132	10.2	18.6	16.3
−122	270	15.6	132	10.3	19.0	16.3

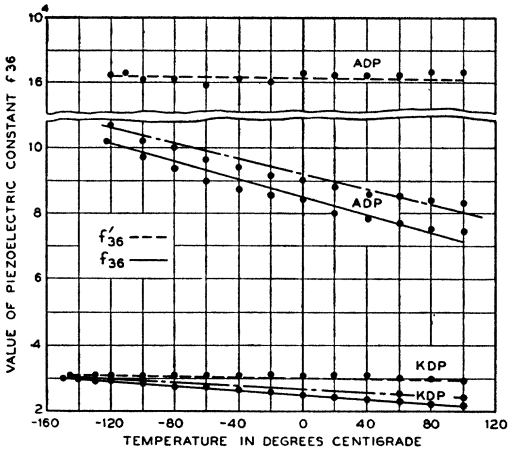

FIG. 15. Values of piezoelectric constant f_{36} for KDP and ADP.

—— Ratio of piezoelectric stress to surface charge σ.
—- Ratio of piezoelectric stress to polarization P.
------ Ratio of piezoelectric stress to dipole polarization P_D.

Since the "free" dielectric constant may be obtained from Fig. 12, and the short circuited compliance modulus is given in the last column of Table II for ADP, all the necessary data are given for determining the piezoelectric constant d_{36}. This is shown tabulated in Table III. From the relations

$$e_{36}=d_{36}/s_{66}^{E};\quad g_{36}=4\pi d_{36}/K_3^F;\quad f_{36}=g_{36}c_{66}^{\sigma}, \tag{25}$$

TABLE IV. Piezoelectric constants of KDP.

Temperature in °C	$d_{36}\times10^8$	$e_{36}\times10^{-4}$	$g_{36}\times10^8$	$f_{36}\times10^{-4}$	K_{33}^C	$f_{36}^*\times10^{-4}$
100	50.4	2.91	36.8	2.16	17.0	2.93
80	54.0	3.17	37.2	2.21	18.0	2.96
60	59.0	3.5	38.6	2.32	18.9	3.05
40	63.2	3.8	38.8	2.35	20.3	3.02
20	69.6	4.26	39.4	2.44	21.8	3.09
0	76.2	4.73	39.6	2.50	23.75	3.09
−20	85.9	5.39	40.4	2.58	26.0	3.13
−40	98.6	6.24	41.0	2.66	29.4	3.12
−60	119.0	7.55	41.5	2.73	34.9	3.12
−80	153.0	9.75	42.0	2.79	43.9	3.10
−100	202	12.8	42.2	2.81	57.6	3.02
−120	334	20.8	43.0	2.93	89.8	3.06
−130	480	29.0	43.2	2.97	123.0	3.07
−140	875	47.3	43.4	2.98	200.0	3.03
−145	1465	70.0	43.6	3.02	291.0	3.06
−150	4400	130.0	44.0	3.07	542.0	3.03

TABLE V.

Frequency	102,250	102,270	102,280	102,290	102,300	102,310	102,320	102,330
Equivalent shunt resistance in ohms	1,200,000	680,000	570,000	500,000	550,000	700,000	900,000	1,180,000

all the forms of the piezoelectric constants are determined and are listed in Table III. The clamped dielectric constants K_3^C can be calculated from this data by means of the formula

$$K_3^C = K_3^F - 4\pi e_{36} d_{36}. \quad (26)$$

This is given in the next to the last column and is shown plotted as the inverse susceptibility in Fig. 12. The corresponding data for KDP are given in Table IV. The inverse susceptibilities of the clamped dielectric constant are plotted by the full lines of Fig. 12. For KDP the values lie on a curve determined by the equation

$$K_3^C = 4.5 + 3100/(T+154.5), \quad (27)$$

indicating that the Curie temperature for the clamped crystal is about 3.5°C lower than for the free crystal. For ADP the equivalent formula is

$$K_3^C = 7.0 + 2560/(T+342). \quad (28)$$

The value of the indicated Curie temperature of -342°C is below absolute zero and indicates that ADP would not be ferroelectric at any temperature.

We note from Tables III and IV that the piezoelectric constant f_{36}, which relates the piezoelectric stress to the charge σ_z, is not a constant independent of temperature. This is shown by the curves of Fig. 15 which show a plot of the constants for ADP and KDP. To test out the supposition that the stress is proportional to that part of the polarization that is temperature variable, use is made of Eq. (12)

$$f_{36}^* = f_{36} K_3^C/(K_3^C - K_{30}). \quad (12)$$

The last column in each table shows a calculation of f_{36}^* and the values for ADP and KDP are plotted by the dotted lines of Fig. 15. For ADP and KDP this supposition appears to be borne out.

Measurements were also made for d_{14} for both ADP and KDP at room temperature. On account of the very small coupling for these modes, the separations of resonant and anti-resonant frequencies of 45° X-cut crystals do not become a very reliable method for measuring the constants. This follows from the fact that the maximum and minimum points for the current through the crystal become more widely separated than they should be if the crystal had no mechanical resistance. In order to determine this constant, a KDP crystal was placed in an impedance bridge and the equivalent shunt resistance was measured as a function of frequency near resonance. The result is shown by Table V for a KDP crystal having the dimension $L=19.56$ mm; $W=6.10$ mm; $T=0.90$ mm. The shunt capacity of the crystal was measured and was found to be 54 $\mu\mu$f agreeing with the dielectric constant of 46 shown in Fig. 11. By considering the equivalent circuit of the crystal given in Fig. 16, it can be shown that the equivalent shunt resistance of the crystal is given by the formula

$$R_S = R_1\left[1+\left(\frac{r}{2\pi f_R R_1 C_0}\right)^2\left(\frac{f_R}{f}-\frac{f}{f_R}\right)^2\right], \quad (29)$$

where R_1 is the shunt resistance at resonance, i.e., the R_1 of Fig. 16, C_0 the shunt capacity of the crystal, r the ratio of C_0 to C_1, and f_R the resonant frequency of the crystal. From the above measurements $R_1=500{,}000$ ohms; $f_R=102{,}290$ cycles; $C_0=54\times10^{-12}$ farad. At 40 cycles from resonance the ratio of $R_s/R_1=2.4$. This gives enough data to solve for r, which we find to be 26,400. From the appendix, we find that the electromechanical coupling factor is

$$k=\left(1\Big/1+\frac{8}{\pi^2 r}\right)^{\frac{1}{2}}=0.00685. \quad (30)$$

From the resonant frequency and the length, s_{22}'

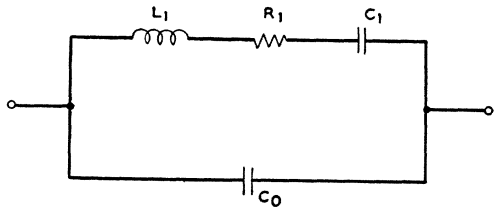

FIG. 16. Equivalent electrical circuit of a crystal.

is found to be 2.56×10^{-12} cm^2/dyne. Hence

$$d_{14}=2\times k(K_1{}^F s_{22}'/4\pi)^{\frac{1}{2}}=4.2\times10^{-8}(\text{KDP}). \quad (31)$$

A similar measurement for a 45°-, X-cut ADP crystal gives

$$d_{14}=5.0\times10^{-8}(\text{ADP}). \quad (32)$$

Hence, although the dielectric constants normal to the X direction are very large, the piezoelectric constants for this direction are very small.

One other effect common to ADP and KDP not previously pointed out is that they have a volume conductance much larger than that for Rochelle salt. For crystals grown from Baker's C.P. grade salt, volume resistivities were measured by H. B. Briggs and J. B. Johnson with the results shown by Fig. 17. By comparing the conductivities between central electrodes compared to conductivities measured between guard rings on the edges, it was established that the surface leakage was negligible compared to the volume leakage provided the crystals were placed in a dry atmosphere. Certain impurities introduced into the crystal lattice have a marked effect in increasing this conductivity as will be discussed in a paper by Holden and Murphy.

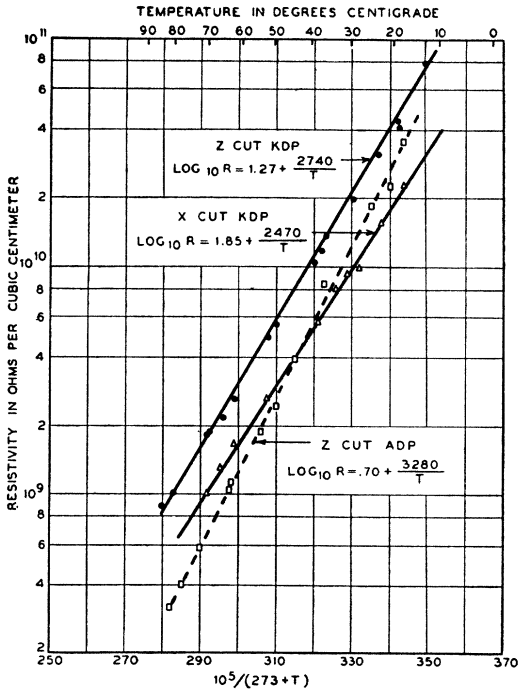

FIG. 17. Specific volume resistivities of ADP and KDP.

V. COMPARISON OF EXPERIMENTAL RESULTS WITH THEORY

The crystal structure of KDP has been worked out by West[14] and is shown by Fig. 18, taken from a paper by Slater,[5] which presents a theory for explaining the ferroelectric properties of KDP. The phosphate groups, PO_4, consist of a phosphorus tetrahedrally surrounded by four oxygens, and are shown by the tetragons. Each phosphate group is surrounded tetrahedrally by four other phosphate groups. The positions of the potassiums in the crystal are shown by the circles. The positions of the hydrogen ions are not shown by x-ray analysis, but according to Slater's model one is located somewhere on the connecting line between each pair of phosphate groups as shown in the figure. The position of these hydrogen ions varies with temperature but most of the time two and only two ions will be near each phosphate group.

Each H_2PO_4 group forms not only an ion but a dipole, and the dielectric behavior shows that the orientation of these dipoles along the $+c$ (or Z) axis or $-c$ axis must have a lower energy than at right angles to it. Hence at very low temperatures, all the dipoles must lie along the Z axis. All the dipoles in one region or "domain" are lined up along the positive Z axis while neighboring domains may have the direction of the dipoles reversed, and thus each domain becomes spontaneously polarized. As the temperature rises the hydrogen ions will acquire a kinetic energy and some of the dipoles will be forced into directions normal to the Z axis. When this condition occurs, the crystal loses its spontaneous polarization. By calculating the number of arrangements of hydrogen when there are N_+, N_0, N_- dipoles pointing along $+Z$, perpendicular to Z and along $-Z$, Slater arrived at an expression for the entropy of the crystal. Combining this with the energy terms, curves for the "free" energy of the crystal are obtained as shown in Fig. 19, where X is a coordinate which measures the net dipole moment of a single domain along the Z axis. It gives directly the dipole moment as a fraction of the maximum or saturation value in the absence of an external

[14] J. West, Zeits. f. Krist. **74**, 306 (1930).

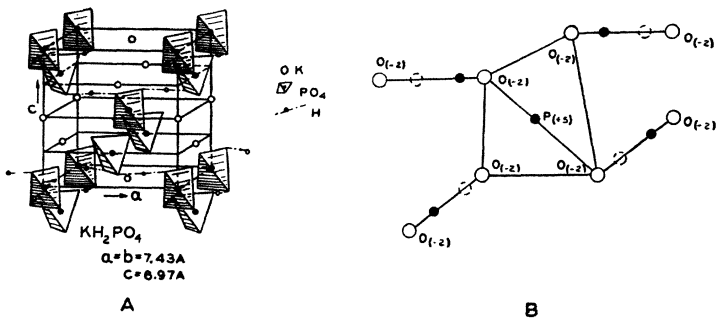

FIG. 18. Crystal structure as determined by x-rays for KDP.

field. The curves of Fig. 19 show that there is one temperature $T=\theta$, the Curie temperature, where the free energy is a straight-line function of X; above this temperature the value of 0 for X has the least free energy, and this corresponds to the condition that the most probable states of the crystal are those arrangements of hydrogens giving a zero net dipole moment and the crystal is unpolarized. Below this temperature, the values of $X=\pm 1$ have the least free energy and the crystal becomes spontaneously polarized in one of the Z directions. When a field is applied in one direction along the Z axis, the equilibrium position shifts from $X=0$ as shown by the dotted lines of Fig. 19, and a polarization results. Slater finds the polarization above the Curie point to be given by the equation

$$P_z=N\mu X=\frac{N\mu^2}{kln2}\frac{E_z}{T-\theta}, \tag{33}$$

where N is the number of molecules per cc, μ the dipole moment of the molecule, k Boltzmann's constant, E_z the applied field, T the temperature, and θ the Curie temperature. Since the dipole moment has been determined from the measurements of Busch[1] to be $\mu=1.25\times10^{-18}$, the susceptibility can be calculated to be

$$\kappa_3=170/(T-\theta). \tag{34}$$

In addition to the susceptibility due to the hydrogen bonds, there is also a susceptibility independent of temperature arising from the polarizability of the other parts of the lattice, principally the oxygens in the phosphate groups. Slater's theory should apply to a single domain below the Curie point and should be applicable to the free dielectric constant above the Curie temperature. From Eq. (17) the free susceptibility

$$\kappa_3^F=\frac{K_3^F-1}{4\pi}=0.279+\frac{249}{T-\theta}, \tag{35}$$

where $\theta=-151$°C for the free crystal. The factor 249 is 1.46 times that calculated, which has been explained by Slater as being due to the extra field produced at the dipoles by the polarizability of the oxygens or other elements. The value of 4.5 for the dielectric constant for these elements alone is not out of line with that obtained for similar crystals.

Slater explains the temperature broadening of the transition (which theoretically should occur at a single temperature) as resulting from stresses set up in the various domains due to the fact that one is polarized and hence sheared in one direction while an adjacent one is polarized in the opposite direction. Hence since different domains are stressed by different amounts, they will have different Curie temperatures, and a continuous transition takes place over a definite temperature range. The maximum theoretical broadening can be calculated from the elastic and piezoelectric data obtained for this paper. One

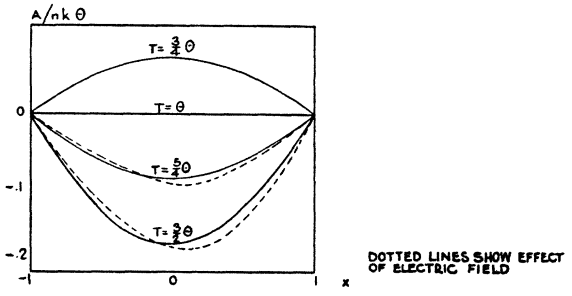

FIG. 19. Slater's free energy curves for KDP.

can show that the temperature shift should be

$$\Delta T = 2(\Delta E/N)/kln2 = 2\Delta E/Nkln2, \quad (36)$$

where ΔE is the increment of free energy per cc and N the number of molecules per cubic centimeter. The change in free energy per cc due to a spontaneous polarization P_z^0 is according to Mueller's theory

$$\Delta E = \tfrac{1}{2}c_{66}^{\sigma}(x_y^0)^2 - f_{36}x_y^0 P_z^0 + \tfrac{1}{2}\chi_3^C(P_z^0)^2 + \tfrac{1}{4}B(P_z^0)^4, \quad (37)$$

where the last term is a non-linear term which for Rochelle salt is small compared to the linear terms. Since the spontaneous polarization (P_z^0) has been measured by Busch to be 4.3×10^{-6} Coulomb per cc $=1.29\times10^4$ c.g.s. units per cc, and g_{36} has been determined to be 44×10^{-8}, a spontaneous shearing strain (x_y^0) should occur for any one domain equal to

$$x_y^0 = g_{36}P_z^0 = 5.65\times10^{-3}. \quad (38)$$

The change in free energy then due to the linear terms in going from a clamped to a free crystal below the curie temperature is

$$\Delta E = \tfrac{1}{2}c_{66}^{\sigma}(x_y^0)^2 - f_{36}(x_y^0)P_z = -1.13\times10^6 \text{ erg per cc.}$$

Hence the temperature range of the transformation should be about

$$\Delta T = 2.29°\text{C},$$

which is somewhat less than the specific heat data[15] and the indicated change of 3.5°C between the clamped and free dielectric constants.

For ADP it appears that two separate systems of hydrogen bonds are involved. Stephenson and Zettlemoyer's[16] measurements on "The Heat Capacity of Ammonium Dihydrogen Phosphate from 15° to 300°K. The Anomaly at the Curie Temperature" indicate that the transition occuring at 148°K (−125°C) is in the nature of a rearrangement of hydrogen bonds. This is confirmed by the fact that a substitution of deuterium for hydrogen raises the transition temperature. On the other hand, the bond system controlling the transition temperature cannot be the same as the H_2PO_4 bond system controlling the dielectric and piezoelectric constants for the data of Figs. 12 and 15 show that there is no deviation from smooth curves as the transition temperature of −125°C is approached. Hence we conclude that the bond system causing the transition temperature is probably due to the four hydrogens in the ammonium ion. These are probably shared with the oxygens in the nearest PO_4 groups, raising the most probable number of hydrogen bonds for each PO_4 group. The sudden shattering of the crystal at −125°C is probably due to a first-order change in crystal structure connected with the ammonium hydrogen bond system. This is indicated by the fact that shattering occurs for ammonium dihydrogen phosphate and ammonium dihydrogen arsenate, but does not occur for potassium dihydrogen phosphate or potassium dihydrogen arsenate. Examples for which the hydrogens of ammonia form bonds affecting the crystal structure are furnished by the crystals ammonium hydrogen fluoride, ammonium azide, and ammonium fluoride.[17]

This ammonium hydrogen bond system may explain why the piezoelectric constant f_{36}* is five times as large in ADP as in KDP, for with the close coupling between all the PO_4 ions that occur through the ammonium hydrogen bonds one would expect a larger change in the lattice positions would be caused by a change in the H_2PO_4 dipoles than would occur in the KH_2PO_4 case, where the PO_4 ions are coupled to the K ions by central electrostatic forces.

By extrapolating the piezoelectric and dielectric constant data to low temperatures, it appears that the piezoelectric Curie temperature should come below absolute zero so that no ferroelectric properties would be expected. This may well be connected with the size of the unit cell which is 7.53A along the a or X axis and 7.542A along the c or Z axis. For KDP, as shown by Fig. 18, the values are 7.43A along X and 6.97A along Z which is associated with the lower energy of the hydrogen bonding system along Z than along X. For ADP, the two are very nearly equal and ferroelectric properties, if any, might be expected to occur along X rather than Z.

[15] C. C. Stephenson and J. G. Hooley, "The heat capacity of potassium dihydrogen phosphate from 15° to 300°K. The anomaly at the Curie temperature," J. Am. Chem. Soc. 66, 1397 (1944).

[16] Stephenson and Zettlemoyer, J. Am. Chem. Soc. 66, 1405–1408 (1944).

[17] See L. Pauling, *Nature of the Chemical Bond* (Cornell University Press, New York, 1944), pp. 299 and 300.

So far, no atomic theories have been developed which allow one to calculate the piezoelectric properties of such crystals as KDP and ADP. Several phenomenological theories have been developed, the most recent of which is the interaction theory of Mueller.[18] The formulation of the theory for small applied fields is similar to that given in Eqs. (4) and (5), except that the polarization P is used in place of the total charge

$$\sigma = P + E/4\pi. \tag{39}$$

For Rochelle salt the conclusion is reached that the open circuited elastic constants show a constant variation with temperature, the piezoelectric constant f_{14}* (for the ferroelectric axis) is independent of temperature, while the only anomaly occurs in the clamped dielectric constant. The same conclusions appear justified for ADP and KDP except that to get an independence of temperature for the piezoelectric constant f_{36}*, we have to take only that part of the polarization which is associated with the dipoles, i.e., the temperature variable part of the dielectric constant. This indicates that it is the shift of the positions of the hydrogen ions which causes the change in the lattice structure and hence the piezoelectric effect. The temperature independence of f_{36}* is shown by Fig. 15. The dielectric constant then provides the only anomaly.

Since no high field measurements have been made, an evaluation of the non-linear terms of Mueller's theory cannot be made.

Note Added in Proof: Recent unpublished measurements by W. A. Yager of this laboratory show that the dielectric constant of ADP remains substantially unchanged from the clamped value up to a frequency of 2.5×10^{10} cycles/sec. (1.2 cm). This result is markedly different from that for ice, which shows marked dispersion at low frequencies, although the mechanism of polarization has been supposed to be similar in both cases (cf. W. Kauzmann, Rev. Mod. Phys. **14**, 12 (1942)). The extremely short relaxation time of ADP is difficult to understand. The mechanism of polarization by motion along hydrogen bonds from one equilibrium position to another seems to be ruled out.

APPENDIX

A-1 Longitudinal Vibrations

In Section IV of the paper use is made of the difference in the resonance frequencies of a plated crystal and a bare crystal to evaluate the piezoelectric coupling factor k of a crystal. An alternate method is to use the frequency separation between resonance and anti-resonance. It is the purpose of this appendix to evaluate these separations as a function of the fundamental constants of an ADP or KDP crystal.

For a plated crystal, the piezoelectric relations of Eqs. (1) are the most useful form. Since only shear piezoelectric constants exist, it is necessary to cut crystals normal to the X or Z axis with their lengths at an angle from the other two axes, in order to generate longitudinal vibrations. Longitudinal vibrations are more advantageous for measuring piezoelectric constants for it is possible to get single modes of motion free from other couplings by using this type of vibration.

To obtain the piezoelectric relations for a 45° Z-cut crystal, for example, it can be shown by tensor transformation, that the equations for a crystal cut normal to Z with its length at an angle θ with the X axis will be

$$\begin{aligned}
-x_x' &= X_x'[s_{11}(\sin^4\theta+\cos^4\theta)+(2s_{12}+s_{66}^E)\sin^2\theta\cos^2\theta] \\
&\quad + Y_y'\left[(2s_{11}-s_{66}^E)\sin^2\theta\cos^2\theta+s_{12}(\sin^4\theta+\cos^4\theta)+\frac{s_{66}^E}{2}\sin 4\theta\right]+Z_z's_{13} \\
&\quad + X_y'\left[\frac{s_{66}^E+2s_{12}-2s_{11}}{2}\sin 4\theta\right]+E_z\frac{d_{36}}{2}\sin 2\theta, \qquad (1) \\
\sigma_z &= \frac{K_3^F}{4\pi}E_z-\frac{d_{36}}{2}[(X_x'-Y_y')\sin 2\theta+X_y'\cos 2\theta],
\end{aligned}$$

where the primes refer to the stresses and strains expressed with respects to the rotated axes.

[18] Reference 6 and H. Mueller, "Properties of Rochelle salt III," Phys. Rev. **58**, 565–573 (1940).

When $\theta=45°$, these equations reduce to

$$-x_x'=X_x'\left[\frac{s_{11}+s_{12}}{2}+\frac{s_{66}^E}{4}\right]+Y_y'\left[\frac{s_{11}+s_{12}}{2}-\frac{s_{66}^E}{4}\right]+Z_z's_{13}+\frac{d_{36}}{2}E_z, \quad (2)$$

$$\sigma_z=\frac{K_3^F}{4\pi}E_z-\frac{d_{36}}{2}(X_x'-Y_y').$$

A pure longitudinal vibration is obtained when the length of the crystal is much greater than the width and thickness dimensions. The stress boundary conditions to be satisfied for a freely vibrating crystal are that all stresses vanish over the surface of the crystal. Since the thickness and width are taken very small and all of the stresses are zero on the surfaces, it follows that no stress can differ appreciably from zero except the stress along the length, X_x'. Hence for such a crystal Eqs. (2) reduce to

$$-x_x'=X_x's_{11}^{E'}+\frac{d_{36}}{2}E_z, \qquad \sigma_z=\frac{K_3^F}{4\pi}E_z-\frac{d_{36}}{2}X_x', \quad (3)$$

where

$$s_{11}^{E'}=\frac{s_{11}+s_{12}}{2}+\frac{s_{66}^E}{4}.$$

The equations of motion can be derived from these equations and Newton's law of motion.

$$F_x=Ma=(\rho\, dxdydz)\frac{d^2\xi}{dt^2}, \quad (4)$$

where M is the mass of an elementary volume $dxdydz$, a the acceleration, and ξ is the displacement of the element in the X' direction.

Let us next consider a small cross section of the crystal with a dimension dx' along the crystal length. The total force on the section is a resultant of the difference in stresses on the two faces or equal to

$$l_wl_t[X_{x_1}'-X_{x_2}']=-l_wl_t\frac{\partial X_x'}{\partial x'}dx'=F_x, \quad (5)$$

where X_x' the stress is considered as a compressional stress acting on the faces of the element. By Newton's law of motion (4) we have

$$-l_wl_tdx'\frac{\partial X_x'}{\partial x'}=l_wl_tdx'\rho\frac{d^2\xi}{dt^2}$$

or

$$\frac{\partial X_x'}{\partial x'}=-\rho\frac{d^2\xi}{dt^2}. \quad (6)$$

For a completely plated crystal such as we are considering, the potential gradient E_z will be independent of the x' direction, since any charge distribution will be equalized with the speed of light which is much higher than the speed of sound in a crystal. Then Eq. (3) when differentiated with respect to x' becomes

$$-\frac{\partial X_x'}{\partial x'}=\frac{1}{s_{11}^{E'}}\frac{\partial x_x'}{\partial x}=\frac{1}{s_{11}^{E'}}\frac{\partial^2\xi}{\partial x'^2}, \quad (7)$$

by the equation of the longitudinal stress X_x'. Introducing this equation into (6), the equation of motion for a plated crystal becomes

$$\frac{\partial^2\xi}{\partial x'^2}=s_{11}^{E'}\rho\frac{d^2\xi}{dt^2}. \quad (8)$$

For simple harmonic motion the variation of ξ with time can be written in the usual form

$$\xi=\xi e^{i\omega t}, \quad (9)$$

so that the simple harmonic motion Eq. (8) becomes

$$\frac{d^2\xi}{dx'^2}-\omega^2\rho s_{11}^{E'}\xi=\frac{d^2\xi}{dx'^2}-\frac{\omega^2}{v^2}\xi=0, \quad (10)$$

where v the velocity of a plated crystal is given by the formula

$$v^2=1/\rho s_{11}^{E'}. \quad (11)$$

A solution of Eq. (10) with two arbitrary boundary conditions is

$$\xi=A\cos\frac{\omega x'}{v}+B\sin\frac{\omega x'}{v}. \quad (12)$$

To determine the constants A and B, use is

made of Eqs. (3). Differentiating (12)

$$-\frac{d\xi}{dx'}=-x_x'=\frac{\omega}{v}\left[A\sin\frac{\omega x'}{v}-B\cos\frac{\omega x'}{v}\right]$$

$$=s_{11}^{E'}X_x'+\frac{d_{36}}{2}E_z. \quad (13)$$

When $x'=0$ and $x'=l$ the bar length, for a free crystal the stress

$$X_x'=0 \text{ when } x'=0 \text{ and } x'=l. \quad (14)$$

Under these conditions

$$-\frac{\omega}{v}B=\frac{d_{36}}{2}E_z$$

and

$$\frac{\omega}{v}\left[A\sin\frac{\omega l}{v}-B\cos\frac{\omega l}{v}\right]=\frac{d_{36}}{2}E_z. \quad (15)$$

Solving these equations for A and B and substituting in (13), we have

$$-x_x'=\frac{d_{36}}{2}E_z\left[\tan\frac{\omega l}{2v}\sin\frac{\omega x'}{v}+\cos\frac{\omega x'}{v}\right]$$

$$=s_{11}^{E'}X_x'+\frac{d_{36}}{2}E_z$$

or

$$x_x'=\frac{-d_{36}E_z}{2s_{11}^{E'}}\left[1-\frac{\cos\dfrac{\omega(x'-l/2)}{v}}{\cos\dfrac{\omega l}{2v}}\right]. \quad (16)$$

The electrical impedance measured at the terminals of a plated crystal is then determined by substituting the value of x_x' in the last of Eqs. (3) and integrating the charge σ over the whole surface. The current into the crystal is then

$$i=j\omega\int\sigma_z dS=j\omega l_w\int_0^l E_z\left[\frac{K_3^F}{4\pi}-\frac{d_{36}^2}{4s_{11}^{E'}}\left(1-\frac{\cos\dfrac{\omega(x'-l/2)}{v}}{\cos\dfrac{\omega l}{2v}}\right)\right]dx'$$

$$=j\omega E_z l_w l\left[\frac{K_3^F}{4\pi}-\frac{d_{36}^2}{4s_{11}^{E'}}\left(1-\frac{\tan\dfrac{\omega l}{2v}}{\dfrac{\omega l}{2v}}\right)\right]=j\omega E_z l_w l\left[\frac{K_3^{LC}}{4\pi}+\frac{d_{36}^2}{4s_{11}^{E'}}\frac{\tan\dfrac{\omega l}{2v}}{\dfrac{\omega l}{2v}}\right], \quad (17)$$

where $K_3^{LC}=K_3^F-\pi d_{36}^2/s_{11}^{E'}$ is called the longitudinally clamped dielectric constant, i.e., the dielectric constant that would be measured if we suppress the longitudinal strain along the x' axis but not the other strains. The admittance of the crystal then is

$$\frac{i}{E}=\frac{i}{E_z l_t}=\frac{j\omega l_w l}{l_t}\left[\frac{K_3^{LC}}{4\pi}+\frac{d_{36}^2}{4s_{11}^{E'}}\frac{\tan\dfrac{\omega l}{2v}}{\dfrac{\omega l}{2v}}\right]. \quad (18)$$

This consists of two terms which represent parallel branches in the equivalent circuit. One of these is the capacitance

$$C_0=\frac{l_w l K_3^{LC}}{4\pi l_t}\text{ c.g.s. units}=\frac{l_w l K_3^{LC}}{4\pi l_t(9\times10^{11})}\text{ farads:} \quad (19)$$

The other branch contains the impedance

$$\frac{-jlt}{\omega l_w l}\left[\frac{4s_{11}^{E'}}{d_{36}^2}\frac{\dfrac{\omega l}{2v}}{\tan\dfrac{\omega l}{2v}}\right]\text{ c.g.s. units}$$

$$=\frac{-jl_t 4s_{11}^{E'}\dfrac{\omega l}{2v}\times9\times10^{11}}{\omega l_w l d_{36}^2\tan\dfrac{\omega l}{2v}}\text{ ohms.} \quad (20)$$

This branch will have a zero impedance or will resonate when the tangent is infinite or when

$$\frac{2\pi f_R l}{2v}=\frac{\pi}{2} \quad \text{or} \quad f_R=\frac{v}{2l}=\frac{1}{2l(\rho s_{11}^{E'})^{\frac{1}{2}}}. \quad (21)$$

Hence for the fully plated crystal it is the zero field elastic constant that determines the resonant frequency.

The anti-resonant frequency (the frequency of highest impedance) is determined by setting Eq. (18) equal to zero and solving for the resultant frequency. This is given by the equation

$$\tan\frac{\omega l}{2v}=-\frac{\omega l}{2v}\left(\frac{4s_{11}^{E'}K_3^{LC}}{4\pi d_{36}^2}\right). \tag{22}$$

Now since

$$K_3^{LC}=K_3^F-\pi d_{36}^2/s_{11}^{E'},$$

this can be written

$$\tan\frac{\omega l}{2v}=-\frac{\omega l}{2v}\left[\frac{4s_{11}^{E'}K_3^F}{4\pi d_{36}^2}\left(1-\frac{4\pi d_{36}^2}{4s_{11}^{E'}K_3^F}\right)\right]=-\frac{\omega l}{2v}\left(\frac{1-k^2}{k^2}\right), \tag{23}$$

by the definition of the coupling.

If the coupling is small, the impedance of Eq. (20) can be represented near the resonant frequency by a series capacitance and inductance having the values

$$C_1=\frac{l_w l}{l_t}\frac{8}{\pi^2}\frac{d_{36}^2}{4s_{11}^{E'}\times 9\times 10^{11}}\text{ farads};$$
$$L_1=4\frac{\rho s_{11}^{E'} l l_t\times 9\times 10^{11}}{8 l_w d_{36}^2}\text{ henries}. \tag{24}$$

Taking the ratio of C_0 to C_1, we have

$$\frac{C_0}{C_1}=r=\frac{\pi^2}{8}\left(\frac{K_3^{LC}s_{11}^{E'}}{\pi d_{36}^2}\right)=\frac{\pi^2}{8}\left(\frac{1-k_2}{k^2}\right). \tag{25}$$

When k is large, this representation is not accurate. Fig. 20 shows a calculation of the ratio of the resonant frequency and anti-resonant frequency to the resonant frequency of an unplated crystal expressed as a function of the coupling k. Hence if the ratio of anti-resonant to resonant frequency is known, the coupling can be evaluated. Similarly if the ratio of the resonant frequency of a plated crystal to the resonant frequency of an unplated crystal is known, the coupling can be evaluated. Care must be taken, however, that the weight of the plating is not sufficient of itself to lower the frequency of the plated crystal. This precaution has been followed in the data given in this paper.

To determine the frequency of an unplated crystal measured mechanically, or electrically in an air gap holder with a large air gap, use can be made of the equations expressed as in Eq. (4) of the body of the paper. For an unplated crystal with all driving plates a long distance away, the electrical boundary conditions are that the surface charges are equal to zero. The effect of any polarization produced by a motion of the crystal is annulled by a depolarizing field

$$E_z=-4\pi P_z. \tag{26}$$

Hence the elastic constants operative are the charge or "open circuited" elastic constants. By tensor transformations, the equations for a 45° Z-cut crystal become

$$-x_x'=X_x'\left[\frac{s_{11}+s_{12}}{2}+\frac{s_{66}^{\sigma}}{4}\right]+Y_y'\left[\frac{s_{11}+s_{12}}{2}-\frac{s_{66}^{\sigma}}{4}\right]+Z_z's_{13}+\frac{g_{36}}{2}\sigma_z, \tag{27}$$
$$E_z=\frac{4\pi\sigma_z}{K_3^F}+\frac{g_{36}}{2}(X_x'-Y_y').$$

For a longitudinal crystal, isolated electrically,

$$Y_y'=Z_z'=\sigma_z=0. \tag{28}$$

Then the equation of motion becomes

$$\frac{\partial^2\xi}{\partial x'^2}=\left(\frac{s_{11}+s_{12}}{2}+\frac{s_{66}^{\sigma}}{4}\right)\rho\frac{d^2\xi}{dt^2}=s_{11}^{\sigma'}\rho\frac{d^2\xi}{dt^2}, \tag{29}$$

and the resonant frequency is determined by the "open circuited" elastic constant $s_{11}'^{\sigma}$. By Eqs. (3) this is related to the short circuited elastic constant

$$s_{11}^{\sigma'}=\frac{s_{11}+s_{12}}{2}+\frac{s_{66}^{\sigma}}{4}=\frac{s_{11}+s_{12}}{2}+\frac{s_{66}^{E}-d_{36}g_{36}}{4}$$
$$=\left(\frac{s_{11}+s_{12}}{2}+\frac{s_{66}^{E}}{4}\right)\left[1-\frac{4\pi d_{36}^2}{4K_3^F\left(\frac{s_{11}+s_{12}}{2}+\frac{s_{66}^{E}}{4}\right)}\right]=s_{11}^{E'}\left[1-\frac{4\pi d_{36}^2}{4K_3^F s_{11}^{E'}}\right]=s_{11}^{E'}(1-k^2). \tag{30}$$

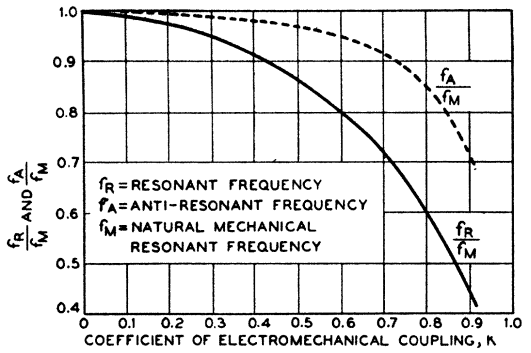

FIG. 20. Ratios of resonant and anti-resonant frequencies to the natural mechanical resonant frequency plotted as a function of the coupling coefficient k.

Hence the ratios of the open circuited to the short circuited frequencies is given by

$$f_0/f_s = 1/(1-k^2)^{\frac{1}{2}} \tag{31}$$

as shown plotted in Fig. 20.

A-2 Face Shear Vibrations

In measuring the shear elastic constants of ADP and KDP, a crystal was used cut normal to the Z or X axes, with its length large compared to its width and very large compared to its thickness. The elastic shear constant was measured by dimensioning the crystal so that no coupling occurred to adjacent flexure modes or by measuring high harmonics of the shear mode. We wish to show that this measurement determines the $c_{66}{}^E$ or $c_{44}{}^E$ elastic constants.

This is a more general contour mode than the longitudinal one considered and involves satisfying boundary conditions along four edges. We consider a Z-cut crystal and assume that the thickness is so small that the stresses determined by the Z direction can be set equal to zero. Hence

$$Z_x = X_z; \quad Z_y = Y_z; \quad Z_z \tag{32}$$

can all be set equal to zero. The remaining stresses

$$X_x, \; X_y, \; Y_y \tag{33}$$

are all finite throughout the crystal but vanish at the edges. The vanishing of the stresses of Eq. (32) simplifies the equations of motion for it results in only three independent strains x_x, x_y, y_y. This is readily seen from Eq. (3) of the body of the paper by setting $Z_s = Y_s = Z_x = E_x = E_y = 0$. Then $y_z = z_x = 0$ and

$$z_z = (c_{13}x_x + c_{13}y_y)/c_{33}.$$

Hence the piezoelectric equations become

$$\begin{aligned} -X_x &= c_{11}{}^* x_x + c_{12}{}^* y_y, \quad c_{11}{}^* = c_{11} - c_{13}{}^2/c_{33}, \\ -Y_y &= c_{12}{}^* x_x + c_{11}{}^* y_y, \quad c_{12}{}^* = c_{12} - c_{13}{}^2/c_{33}, \\ -X_y &= c_{66}{}^E x_y - e_{36} E_z, \\ \sigma_z &= \frac{K_3{}^C}{4\pi} E_z + e_{36} x_y. \end{aligned} \tag{34}$$

Newton's equations of motion for a two-dimension crystal become

$$\begin{aligned} \rho \frac{d^2\xi_1}{dt^2} &= -\frac{\partial X_x}{\partial x} - \frac{\partial X_y}{\partial y} = c_{11}{}^* \frac{\partial x_x}{\partial x} + c_{12}{}^* \frac{\partial y_y}{\partial x} \\ &\quad + c_{66}{}^E \frac{\partial x_y}{\partial y} - e_{36} \frac{\partial E_z}{\partial y}, \\ \rho \frac{d^2\xi_2}{dt^2} &= -\frac{\partial Y_x}{\partial x} - \frac{\partial Y_y}{\partial y} = c_{66}{}^E \frac{\partial x_y}{\partial x} + c_{12}{}^* \frac{\partial x_x}{\partial y} \\ &\quad + c_{11}{}^* \frac{\partial y_y}{\partial y} - e_{36} \frac{\partial E_z}{\partial x}, \end{aligned} \tag{35}$$

where ξ_1 and ξ_2 are the displacements along X and Y at any point. Since the plating is an equipotential surface $\partial E_z/\partial x = \partial E_z/\partial y = 0$. Also by the definition of the strains

$$x_x = \frac{\partial \xi_1}{\partial x}; \quad y_y = \frac{\partial \xi_2}{\partial y}; \quad x_y = \frac{\partial \xi_1}{\partial y} + \frac{\partial \xi_2}{\partial x}. \tag{36}$$

Hence for simple harmonic motion, Eqs. (35) become

$$\begin{aligned} &c_{11}{}^* \frac{\partial^2 \xi_1}{\partial x^2} + c_{12}{}^* \frac{\partial^2 \xi_2}{\partial x \partial y} \\ &\quad + c_{66}{}^E \left[\frac{\partial^2 \xi_1}{\partial y^2} + \frac{\partial^2 \xi_2}{\partial x \partial y} \right] + \omega^2 \rho \xi_1 = 0, \\ &c_{66}{}^E \left[\frac{\partial^2 \xi_1}{\partial x \partial y} + \frac{\partial^2 \xi_2}{\partial x^2} \right] + c_{12}{}^* \frac{\partial^2 \xi_1}{\partial x \partial y} \\ &\quad + c_{11}{}^* \frac{\partial^2 \xi_2}{\partial y^2} + \omega^2 \rho \xi_2 = 0. \end{aligned} \tag{37}$$

We wish to show that when the crystal is very long in the X direction compared to its width in the Y direction, the shearing resonant frequency will be controlled by the $c_{66}{}^E$ elastic constant.

To show this let

$$\xi_1 = A \sin hy; \quad \xi_2 = 0. \tag{38}$$

This satisfies Eq. (37) provided that

$$h = \omega(\rho/c_{66}^E)^{\frac{1}{2}} = \omega/v, \tag{39}$$

where v is the velocity of propagation of a shear wave. The X_x and Y_y stresses vanish identically over the crystal. To make X_y vanish when $y = \pm l_w/2$ we have

$$\begin{aligned} -X_y &= c_{66}^E\left(\frac{\partial \xi_1}{\partial y} + \frac{\partial \xi_2}{\partial x}\right) - e_{36}E_z \\ &= A\omega(\rho C_{66}^E)^{\frac{1}{2}} \cos\frac{\omega y}{v} - e_{36}E_z, \\ &= 0 \quad \text{when} \quad y = \pm l_w/2. \end{aligned} \tag{40}$$

Hence

$$A = \frac{e_{36}E_z}{\omega(\rho c_{66}^E)^{\frac{1}{2}} \cos \omega l_w/2v}$$

and

$$\begin{aligned} \xi_1 &= \frac{e_{36}E_z \sin \omega y/v}{\omega(\rho c_{66}^E)^{\frac{1}{2}} \cos \omega l_w/2v}; \\ X_y &= e_{36}E_z\left[\frac{\cos \omega y/v}{\cos \omega l_w/2v} - 1\right]; \quad X_x = Y_y = 0. \end{aligned} \tag{41}$$

Hence all the boundary conditions are satisfied except for X_y at $x = \pm l/2$. Here the shear stress puts in a force in the y direction which when integrated over the surface becomes

$$F_y = e_{36}E_z l_w l_t\left[\frac{\tan \omega l_w/2v}{\omega l_w/2v} - 1\right] \text{ at } x = \pm\frac{l}{2}. \tag{42}$$

This is the type of force that will tend to drive an even order flexure in the bar. As the length l increases with respect to the width l_w, it can be shown that the amplitude of the flexure motion approaches zero for a constant driving force, so that for a crystal long compared to its width, the solution given above is approached. Hence a harmonic of a shear mode for a long narrow crystal approaches this condition very closely. Such modes can therefore be used to evaluate the shear elastic constants c_{66}^E and c_{44}^E.

The impedance of a long narrow shear vibrating crystal can be derived from the last of Eqs.

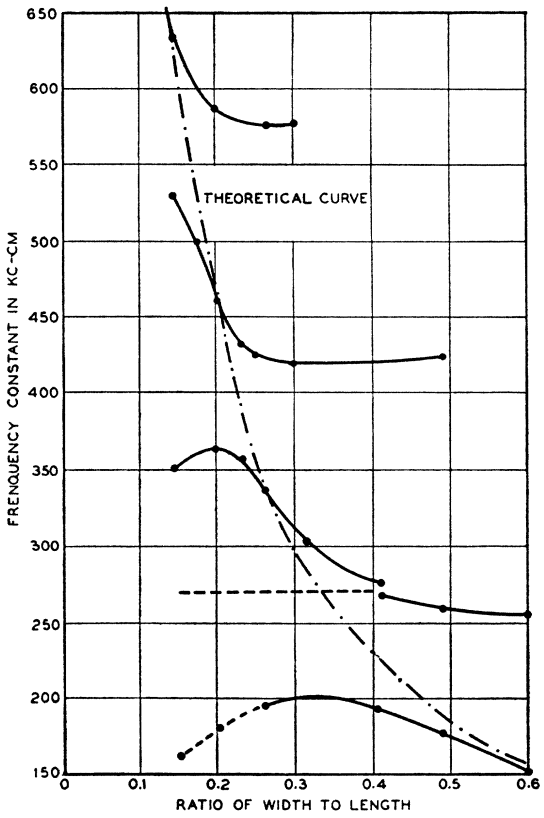

FIG. 21. Frequency spectrum of a Z-cut ADP crystal vibrating in shear.

(34) by integrating the charge over the surface of the crystal. Since

$$x_y = \frac{e_{36}E_z}{c_{66}^E}\frac{\cos \omega y/v}{\cos \omega l_w/2v}, \tag{43}$$

we find

$$\begin{aligned} Q &= \int_{-l/2}^{l/2} dx \int_{-l_w/2}^{l_w/2} \sigma_z dy \\ &= E_z l l_w\left[\frac{K_3{}^C}{4\pi} + \frac{e_{36}{}^2}{c_{66}^E}\frac{\tan \omega l_w/2v}{\omega l_w/2v}\right] = \frac{i}{j\omega}. \end{aligned} \tag{44}$$

In a similar manner to that discussed for the longitudinal crystal, we can show that the resonance occurs when

$$f_R = \frac{1}{2l_w}\left(\frac{c_{66}^E}{\rho}\right)^{\frac{1}{2}} \tag{45}$$

and that the impedance of the crystal is represented by the equivalent circuit of Fig. 16, with

the constants

$$C_0=\frac{K_3{}^C l_w l}{4\pi l_t(9\times10^{11})}\text{ farads};$$

$$C_1=\frac{8}{\pi^2}\frac{ll_w}{l_t}\left(\frac{e_{36}{}^2}{c_{66}{}^E}\right)\times\frac{1}{9\times10^{11}}\text{ farads};\qquad(46)$$

$$L_1=\frac{\rho ll_t\times9\times10^{11}}{8l_w e_{36}{}^2}\text{ henries.}$$

Hence the ratio of capacities becomes

$$\frac{C_0}{C_1}=r=\frac{\pi^2}{8}\left(\frac{K_3{}^C c_{66}{}^E}{4\pi e_{36}{}^2}\right)=\frac{\pi^2}{8}\frac{(1-k^2)}{k^2},\qquad(47)$$

where k the coefficient of coupling for a shear mode is

$$k^2=\frac{4\pi e_{36}{}^2}{K_3{}^F c_{66}{}^E}=\frac{4\pi d_{36}{}^2}{K_3{}^F s_{66}{}^E}$$

and

$$K_3{}^C=K_3{}^F-4\pi d_{36}e_{36}.\qquad(48)$$

When a crystal is not long compared to its width, the unbalanced forces in the X direction will couple the shear mode to even order flexure modes. This is shown experimentally by Fig. 21, which shows the frequency spectrum of a Z-cut ADP crystal as a function of the ratio of width to length. The main modes can be identified as even order flexures coupled to the shear mode. At certain ratios of width to length the shear and flexure modes coincide and a coupled frequency curve is observed. Midway between couplings, a good agreement is obtained with the frequency calculated from (45). The smaller the ratio of width to length, the better the agreement obtained, as shown by the dotted line which shows the calculated value.